RESEARCH ARTICLE

Proteomic evaluation of wound-healing processes in potato (*Solanum tuberosum* L.) tuber tissue

Inês Chaves[1*], *Carla Pinheiro*[1*], *Jorge A. P. Paiva*[1,2], *Sébastien Planchon*[3], *Kjell Sergeant*[3], *Jenny Renaut*[3], *José A. Graça*[4], *Gonçalo Costa*[1], *Ana V. Coelho*[1,5] *and Cândido P. Pinto Ricardo*[1,4]

[1] Instituto de Tecnologia Química e Biológica (Universidade Nova de Lisboa), Portugal
[2] Tropical Research Institute of Portugal (IICT), Forest and Forest Products Centre, Tapada da Ajuda, Portugal
[3] Centre de Recherche Public – Gabriel Lippmann, Department of Environment and Agrobiotechnologies (EVA), Proteomic Plateform, Luxembourg
[4] Instituto Superior de Agronomia, Tapada da Ajuda, Portugal
[5] Universidade de Évora, Colégio Luís Verney, Portugal

Received: October 9, 2007
Revised: May 6, 2009
Accepted: June 8, 2009

Proteins from potato (*Solanum tuberosum* L.) tuber slices, related to the wound-healing process, were separated by 2-DE and identified by an MS analysis in MS and MS/MS mode. Slicing triggered differentiation processes that lead to changes in metabolism, activation of defence and cell-wall reinforcement. Proteins related to storage, cell growth and division, cell structure, signal transduction, energy production, disease/defence mechanisms and secondary metabolism were detected. Image analysis of the 2-DE gels revealed a time-dependent change in the complexity of the polypeptide patterns. By microscopic observation the polyalyphatic domain of suberin was clearly visible by D4, indicating that a closing layer (primary suberisation) was formed by then. A PCA of the six sampling dates revealed two time phases, D0–D2 and D4–D8, with a border position between D2 and D4. Moreover, a PCA of differentially expressed proteins indicated the existence of a succession of proteomic events leading to wound-periderm reconstruction. Some late-expressed proteins (D6–D8), including a suberisation-associated anionic peroxidase, have also been identified in the native periderm. Despite this, protein patterns of D8 slices and native periderm were still different, suggesting that the processes of wound-periderm formation are extended in time and not fully equivalent. The information presented in this study gives clues for further work on wound healing-periderm formation processes.

Keywords:
MS protein sequencing / Native periderm / Plant proteomics / Potato slices/ *Solanum tuberosum* / Wounding

1 Introduction

Potato (*Solanum tuberosum* L.) is a very important food crop consumed worldwide during extended periods of the year (http://www.cgiar.org/impact/research/potato.html.) and, so, the conservation of the tubers is of high economic importance. The interaction of plant organs, such as the tubers, with the environment is dependent on the epidermis/periderm and many physiological processes are directly or indirectly affected by the characteristics of this structure. The native periderm protects the tubers from pathogen and pest attack [1, 2], dehydration, bruising during harvest and handling and pressure increase during silo storage [3].

Correspondence: Professor Cândido P. Pinto Ricardo, Instituto de Tecnologia Química e Biológica / Universidade Nova de Lisboa, Av. da República-EAN, 2780-157 Oeiras, Portugal
E-mail: ricardo@itqb.unl.pt
Fax: +351-214433644

Abbreviation: UNA, unassigned

*These authors contributed equally to the work.

The ability to rapidly produce a wound-periderm, upon damage, is vital for maintenance of tuber quality [4, 5]. The wound-healing process involves dedifferentiation processes, with activation of metabolism, the formation of mechanical barriers (*e.g.* suberin) [1, 3] and the activation of defensive mechanisms (*e.g.* formation of PR-like proteins) [6].

The response of plant tissues to wounding has been studied for a very long time [7–9] and more recently it has been demonstrated that several genes are wound-inducible [10]. Functional genomics can provide a fundamental insight into the organism development [11] and the responses to stress [12]. The proteomic approach is a very powerful tool to study the protein patterns that result from differential gene expression as well as from post-translational modifications [13]. Although there have been some studies on the potato tuber proteome [14–17] they were not concerned with the wound-healing process.

Potato tuber slices constitute a good model to study wound-induced metabolism [9, 18] and healing [5] and are used in the present work to detect proteins that are sequentially expressed upon excision, leading to suberisation. Proteins were separated by 2-DE and identified by MS techniques, giving information on the sequence of events that take place during healing.

2 Materials and methods

2.1 Plant material

Dormant potato tubers (*S. tuberosum* L.), cv. Asterix, 3 months from harvesting, with fully mature native periderm and free of any visible disease symptoms were bought locally. The tubers' surfaces were washed in running deionised water, for 5 min, followed by 10% commercial bleach, for 10 min and 70% ethanol for 3 min. Five tubers, that constitute the five biological replicates, were peeled and cut into slices (approximately 4 cm in diameter and 1 mm thick), which were suspended by a plastic thread in a wet chamber in the dark at 25°C. Samples of slices from each tuber were collected at 24-h intervals, frozen in liquid nitrogen and stored at −80°C until use. Samples of tuber native periderm (about 0.5 mm thick) were also collected and immediately frozen.

2.2 Microscopic observations

Pieces of tuber slices (approximately 5 mm × 5 mm × 1 mm) were fixed in a solution of 5% formaldehyde, 5% acetic acid and 50% ethanol, dehydrated with an ethanol series, at room temperature, infiltrated in paraplast (Merck) and embedded in paraffin (Histosec-Merck), according to the manufacturer's instructions. Sections (about 10 μm thick) were cut utilizing a rotating microtome (LEICA Instruments). After deparafination and hydration, cuts were stained using Sudan IV to visualise suberin aliphatic domains of the cell walls [19].

2.3 Protein extraction

The plant material (1.5 g samples) was homogenised with 0.6 g of PVPP in liquid nitrogen and suspended in 13 mL of 10% TCA and 60 mM DTT in acetone, at −20°C. The homogenate was centrifuged at 15 000 × *g* for 15 min at 4°C and the pellet recovered and washed with a solution of 60 mM DTT in acetone for 1 h, at −20°C. After centrifugation (at 15 000 × *g* for 15 min at 4°C) the pellet was dried under vacuum and total proteins were extracted by stirring for 2 h at 25°C, in a buffer containing 8 M urea, 4% CHAPS, 2% PVPP and 1% IPG buffer, pH 3–10. The protein was quantified using the Bradford assay, modified by Ramagli [20].

2.4 2-DE

IEF was performed in 24 cm gels, linear pH gradient of 3 to 10 (IPG strips – Amersham Biosiences) that were loaded with 650 μg of total protein. IEF was carried out in a IPGphor isoelectric focusing unit (Amersham Biosiences) at 20°C, with the current limited to 50 μA/strip, according to the following protocol: 9 h of rehydration, followed by 50 V for 10 h, 200 V for 200 Vh, 500 V for 750 Vh, 1000 V for 1500 Vh, 8000 V at a gradient of 6000 Vh and 8000 V up to a total of 80 000 Vh. Following IEF, the proteins in the strips were reduced with DTT and alkylated with iodoacetamide and next separated by SDS-PAGE, in 25 mm × 20 mm × 1 mm gels with a homogeneous acrylamide percentage (%T = 12%, %C = 3.3%). The protein migration took place at constant voltage of 12 V *per* gel, for 14 h, at 15°C. The gels were stained with colloidal blue [21].

2.5 2-DE gel image analysis and statistical analysis

The gels were scanned in the ImageScanner II (Amersham Biosciences) and the images were analysed by REDFIN software from Ludesi (Uppsala, Sweden). The analysis consisted in determining the spots present in each gel, their level of expression and comparing the profiles obtained. Five gels from five different tubers (biological replicates) were made for each sampling date: 0 (D0), 1 (D1), 2 (D2), 4 (D4), 6 (D6) and 8 (D8) days from slicing. Image analysis and spot volume quantification were performed with REDFIN software (Ludesi) and only the spots present in the gels of at least three replicates were accounted for (a total of 1190). Spots selected for statistical analyses ($n = 182$) were those that had a volume ≥ 150 (REDFIN units).

The following ANOVA model was then applied to each spot i on normalised volume values to test the day effect on

protein expression:

$$Y_{ijk} = \mu + D_j + \varepsilon_{ijk}$$

(Y_{ijk}, the normalised volume of spot i ($i = 1$–182) in sample j for replicate k; μ the general mean; D_j, the day effect (j = day 0, day 1, day 2, day 4, day 6 and day 8); ε_{ijk}, the residual of the declared model ($k = 1$–5).

ANOVA were performed using R (R Development Core Team 2004) by means of limma R library (2005) [22]. A spot was classified as differentially expressed between the different data samples if its false discovery rate (FDR) adjusted p-value [23] was <0.05 (96 spots). PCA was performed using the ade4 library of the R package [24] to summarise and explore the relationships existing between differentially expressed proteins along the experiment.

2.6 Protein identification and database search

Spots of interest were excised from colloidal Coomassie Blue-stained gels and processed according to a previously published protocol [25]. An Ettan Spot Handling workstation (GE-Healthcare, Uppsala, Sweden) was used for destaining and tryptic digestion of the gel-separated proteins. Since modules for further sample handling and spotting on MALDI-target plates are integrated in the same instrument, a completely hands-free approach was performed. After spotting of the samples, an MS analysis in MS and MS/MS-mode using a 4800 MALDI TOF/TOF, externally calibrated as outlined by the manufacturer (Applied Biosystems, Foster City, CA), was done. *Per* spot one MS and eight MS/MS spectra of the most intense peaks were automatically acquired.

The acquired MS and MS/MS spectra of each spot were submitted as a single query in database searches against the NCBI database limited to the taxonomical class of the viridiplantae (download from www.ncbi.nlm.nih.gov on 11/01/2008, containing 5 828 094 sequences). The searches were done using the Applied Biosystems GPS software on an in-house MASCOT platform. Similarly, the spectra were searched using an EST database containing all NCBI entries from *S. tuberosum*, downloaded on 22/01/2008. The results of these searches were combined, thereby increasing the number of proteins that could be identified with significance. All identifications were manually verified. For spots that did not result in a significant identification, more peptides were manually selected for fragmentation and, if required, peptide sequences were determined manually and used for homology searches with the FASTS-algorithm (http://fasta.bioch.virginia.edu/fasta_www/cgi/) [26]. Because it is impossible to discern the isobaric amino acids Ile and Leu, all mass increments of 113 Da were arbitrarily designated as Ile. Similarly, mass increments of 128 Da were always denoted as Gln, unless at the C-terminal position of a peptide when Lys was used. To avoid haphazard identifications, a threshold of 10×10^{-4} was rigorously used and a protein was only considered to be identified if the majority of proteins with a significant search score had an identical function [27].

3 Results

3.1 Microscopic observation

Light microscopic observations of the potato tuber slices revealed structural changes in the cell walls during the wound-healing process. Using the Sudan IV stain the cell walls started to be coloured red by D_4 from slicing (Fig. 1), indicating that the deposition of the polyaliphatic domain of suberin had been initiated. Wound-induced suberisation of the tuber tissue involves two stages, during which two types of cells are suberised: 1st stage – formation of a ''closing layer'' (primary suberisation) when walls of the existing parenchyma cells at the wound site suberise; 2nd stage – formation of a ''wound periderm'' (secondary suberisation) when new cells originating from a newly formed phellogen, bellow the closing layer, are suberised [3].

3.2 2-DE polypeptide patterns

To study the changes in proteins associated with the wound-healing process of the potato slices, 2-DE gels for the six

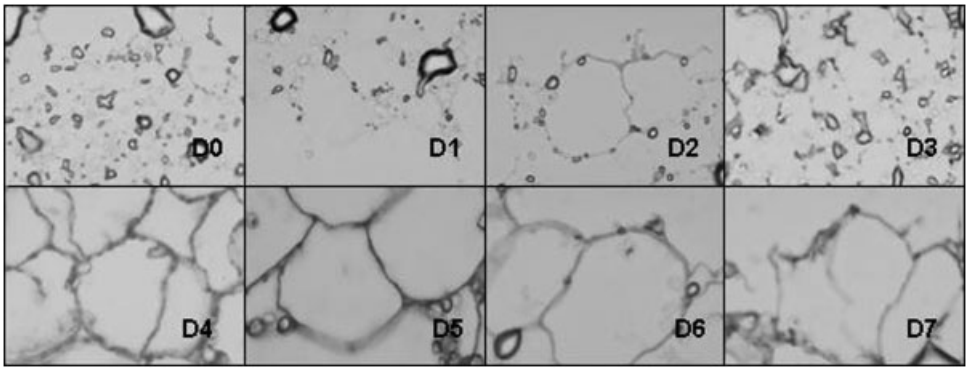

Figure 1. Microscopic observation of potato tuber slices stained with Sudan IV to evidence suberin deposition on the cell walls, during the wound-healing process. D0 to D7 indicate the day after slice cutting; from the 4th day onwards the staining of the polyaliphatic domain of suberin just formed allows the visualisation of the cell contours. This information is consistent with the time course detailed by Lulai and Corsini [40].

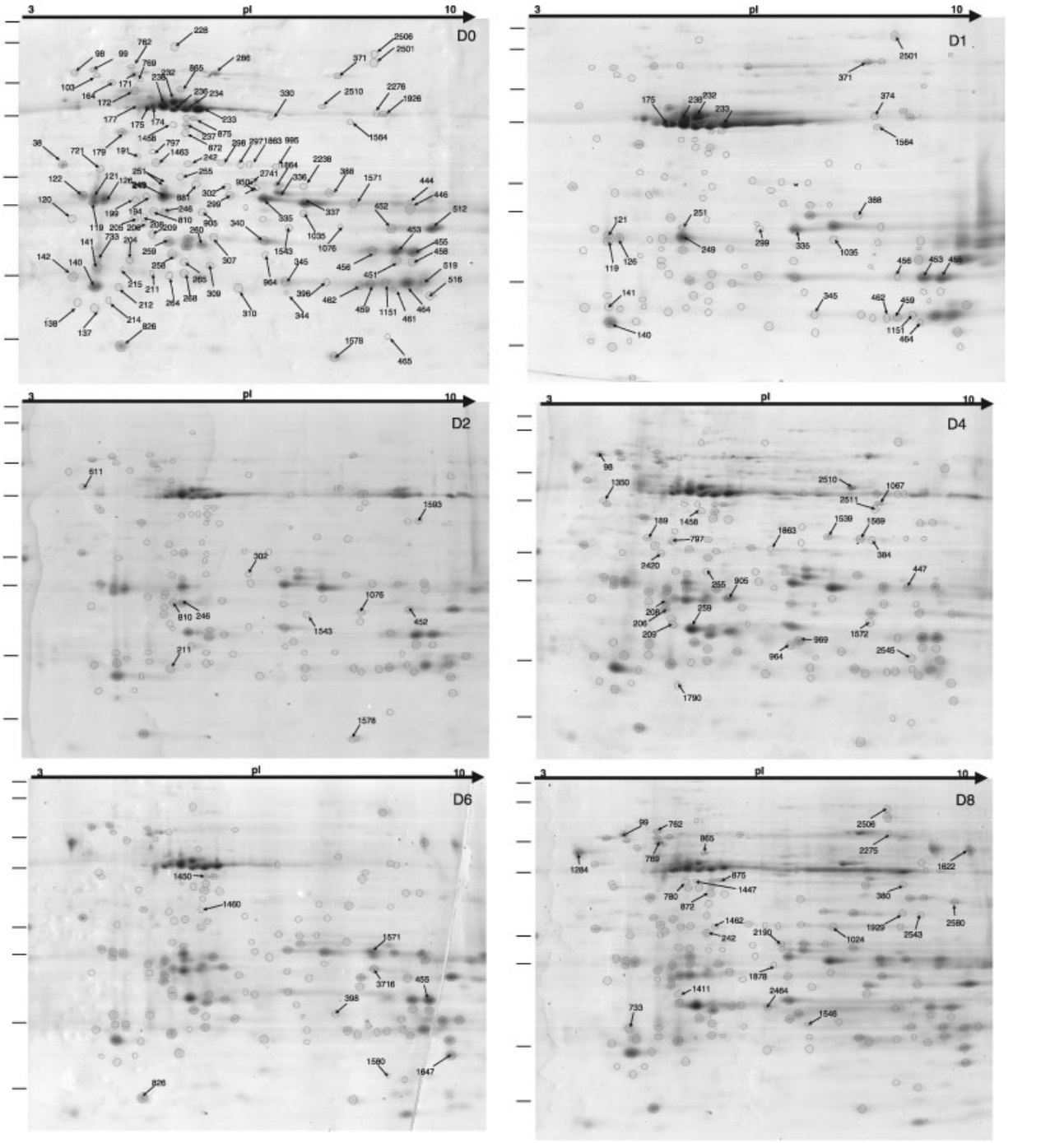

Figure 2. Identification by MS of wound-induced proteins from potato tuber slices resolved on 2-DE gels. D0 to D8 indicate the day after slice cutting. The proteins selected for identification are numbered in the gels. MW markers, respectively, of 100, 75, 50, 37, 25, 20, 15 and 10 kDa, are indicated at the left gel border.

sampling dates (D0, D1, D2, D4, D6 and D8) were run (Fig. 2). Image analysis of the gel patterns was performed using REDFIN software (Ludesi) in order to get polypeptide spot quantification, normalisation and matching. A re-arrangement of the polypeptide patterns was observed as a consequence of wounding, as indicated by the fact that several spots decreased or increased in intensity and others became evident.

Since the wound-healing process leads to the formation of a new periderm (wound periderm) we also performed a 2-DE protein analysis of potato native periderm (Fig. 3) to allow a comparison with the last stages of slice healing.

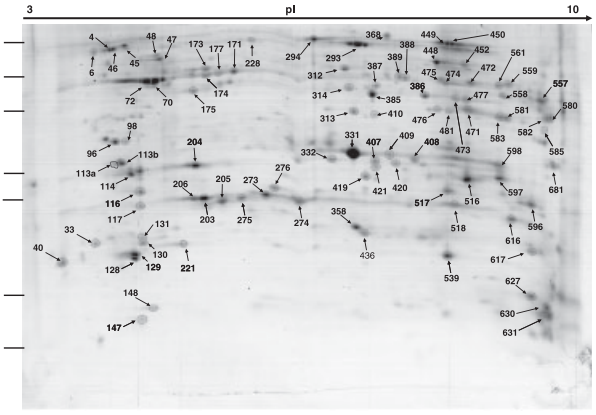

Figure 3. Identification by MS of potato tuber native periderm resolved on 2-DE gels. The proteins selected for identification are numbered in the gel. MW markers, respectively, of 100, 75, 50, 37, 25, 20, 15 and 10 kDa, are indicated at the left gel border.

The patterns of these gels were found to be dissimilar from those of the slices, which precluded a joint image analysis.

3.3 Protein identification in the slices

For the identification in the slices of polypeptides associated with the wound-healing process (D0, D1, D2, D4, D6 and D8 gels) only spots present in at least three replicates (three distinct tubers) and that had a volume ≥ 150 (REDFIN volume units) were considered and excised for MS identification (182 spots analysed and about 90% identified). The results are shown in Table 1 (spots with a p-value < 0.05) and Table S1 (Supporting Information material with additional information about all the spots analysed).

The major proteins that were identified can be grouped in several of the functional categories defined by Bevan *et al.* [28], namely: metabolism, energy, transcription, protein synthesis, protein destination and storage, transporters, cell structure, signal transduction, disease/defence and secondary metabolism. However, a few spots could not be identified and others referred to proteins of unknown function.

Disease/defence appears to be the most represented of the functional classes. Membrane proteins were underrepresented among the identified proteins, with a few exceptions (*e.g.* vacuolar ATPase subunit, mitochondrial porin-like protein, plasma membrane polypeptide, β-subunit of K^+ channels), possibly as a consequence of the general poor solubilisation of such proteins.

3.4 Differentially expressed proteins

Slices polypeptide spots statistically classified as differentially expressed between the several data samples (p-value < 0.05; 96 spots) were subjected to a PCA, so that the relationships existing between the differentially expressed proteins along the experiment could be explored. The PCA accounted for about 85% of the total variance (61.16, 14.36 and 9.28%, respectively for the PC1, PC2 and PC3 axes). As shown in the main PCA plane (PC1–PC2 representation) (Fig. 4A) the six sampling dates originated six distinct entities, which by their position can be considered to define two groups: D0, D1, D2 and D4, D6, D8, with a border line somehow placed between D2 and D4. Such grouping suggests that a sequence of metabolic processes had occurred with time.

The polypeptide spots that are more strongly associated with the PC1 and PC2 axes are indicated on the correlation circle on the PC1–PC2 plane (Fig. 4B). For PC1 those polypeptides are: high molecular weight patatins (♯175, ♯238, ♯233, ♯232) and several protease inhibitors (♯456, ♯459, ♯126, ♯335, ♯119, ♯453, ♯251, *etc.*), when considering the negative half of the axis (early wound-healing events); PR10 (♯259, ♯209), formate dehydrogenase (♯2510), wound-induced protein with a chitin binding domain (♯1076, ♯1572), chitinases (♯1569, ♯1539, ♯242, ♯1929), several protease inhibitors (♯1647, ♯1571, ♯2545, ♯211, ♯3716, ♯1790, *etc.*), peroxidases (♯1284, ♯1622, ♯1593) and low molecular weight patatins (♯2458, ♯208), for the positive half of the axis (late wound-healing events). Proteins that mainly define PC2 are: chitinase (♯384), for the negative half-axis; catalase (♯935) and annexin (♯875) for the positive half-axis.

The proteins that associate most specifically with the initial tuber tissue (D0) are those with $PC1 < -0.6$ and $PC2 \approx 0$, essentially, several protease inhibitors (♯456, ♯459, ♯335, ♯453) and high molecular mass patatins (♯175, ♯238, ♯233, ♯232). For the extreme of our wound-healing experiment (D8) the associated proteins are those with $0.6 > PC1 > 0.9$ and $0.3 > PC2 > 0.7$, namely, peroxidase (♯780), chitinases (♯242, ♯1929), and also proteins like, metacaspase (♯762), annexin (♯1450), EIG-J7 protein (♯1546), Ran protein (♯1024) and proteosoma alfa-subunit (♯1462).

An interesting observation was that proteins of similarly attributed function could have maximum expression at different sampling dates, as it is quite evident for the patatins and the protease inhibitors. In what concerns the inhibitors we identified a great diversity of them. Different designations have been utilised in the databases and the nomenclature is a bit confusing, but by the combined use of the NCBI BLAST and the Merops databases (http://merops.sanger.ac.uk/) [29] we were able to group the several protease inhibitors of the slices in the Merops families I03 and I20. As shown in Fig. 5, the I03 inhibitors could be further divided into the following four classes: 002, 017, 020 and unassigned (UNA). In general, the I03.017 and I03.UNA inhibitors (as well as the I20) had a high expression at D0 that decreased along the wound-healing process, while inhibitors of the other three I03 classes either had an opposite behaviour or remained high for most of the time.

Table 1. List of proteins from the wound-healing potato slices identified by MS and previously separated by 2-DE, with *p*-value ≤ 0.05.

Spot number	Variation of normalised volume (affected by s.d.)	Protein identification	*p*-Value	Functional category
98	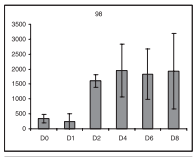	Calreticulin	0.030	Disease/defense
99	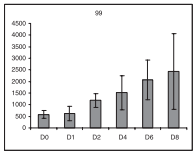	Unnamed protein product	0.034	Unclassified
119	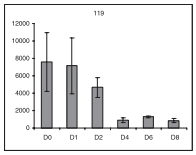	Proteinase inhibitor S9C11 – Merops family I03.017	0.001	Disease/defense
121	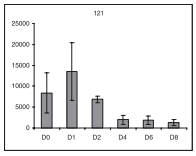	Proteinase inhibitor S9C11 – Merops family I03.017	0.000	Disease/defense
126	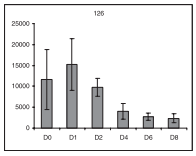	Proteinase inhibitor S9C11 – Merops family I03.017	0.001	Disease/defense
140	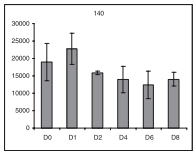	Proteinase inhibitor homologue – Merops family I03.017	0.006	Disease/defense
141	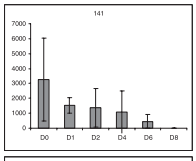	Proteinase inhibitor homologue – Merops family I03.017	0.011	Disease/defense
175	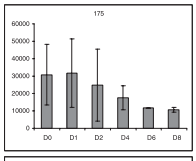	Patatin	0.003	Protein destination and storage
189	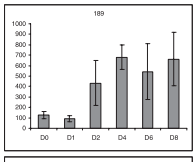	GST	0.008	Disease/defense
206	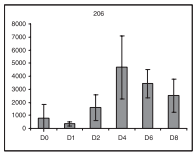	Patatin	0.002	Protein destination and storage

Table 1. Continued

Spot number	Variation of normalised volume (affected by s.d.)	Protein identification	*p*-Value	Functional category
208	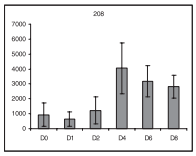	Patatin	0.001	Protein destination and storage
209	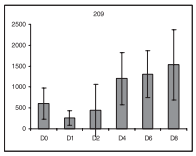	Pathogenesis-related protein 10	0.018	Disease/defense
211	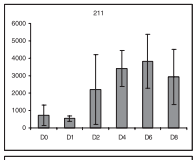	Proteinase inhibitor precursor – Merops family I03.020	0.004	Disease/defense
232	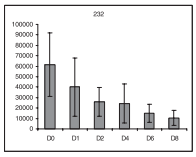	Patatin	0.013	Protein destination and storage
233	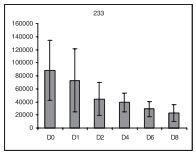	Patatin	0.028	Protein destination and storage
238	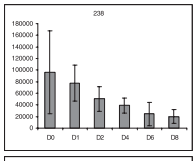	Patatin	0.024	Protein destination and storage
242	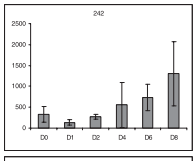	Class II chitinase	0.008	Disease/defense
246	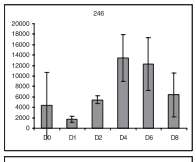	Patatin	0.008	Disease/defense
249	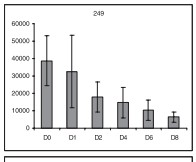	Miraculin (low homology) – Merops family I03.UNA	0.004	Disease/defense
251	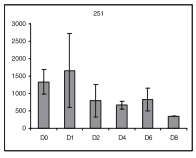	Miraculin (low homology) – Merops family I03.UNA	0.001	Disease/defense

Table 1. Continued

Spot number	Variation of normalised volume (affected by s.d.)	Protein identification	*p*-Value	Functional category
255	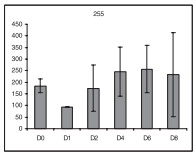	Glycine-rich protein 2	0.000	Disease/defense
259	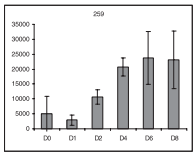	Pathogenesis-related protein 10	0.000	Disease/defense
299	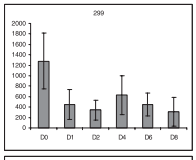	Miraculin (low homology) – Merops family I03.UNA	0.008	Disease/defense
302	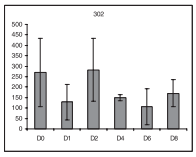	Gamma interferon-responsive lysosomal thiol reductase	0.040	Disease/defense
335	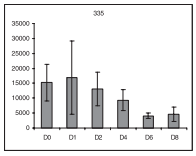	Proteinase inhibitor homologue – Merops family I03.017	0.026	Disease/defense
345	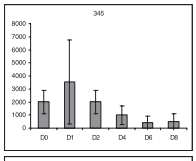	Proteinase inhibitor II – Merops family I20.001	0.043	Disease/defense
371	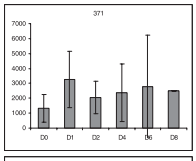	Catalase isozyme 1-like protein	0.004	Disease/defense
374	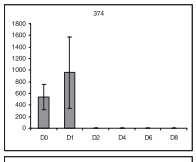	Patatin	0.000	Protein destination and storage
380	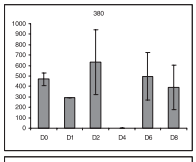	Not identified	0.000	
384	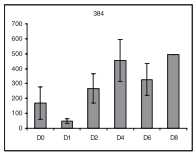	Endochitinase 2	0.002	Disease/defense

Table 1. Continued

Spot number	Variation of normalised volume (affected by s.d.)	Protein identification	*p*-Value	Functional category
388	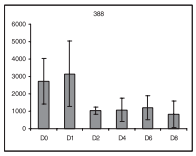	Proteinase inhibitor homologue – Merops family I03.017	0.021	Disease/defense
398	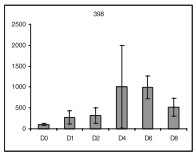	Proteinase inhibitor – Merops family I03.002	0.026	Disease/defense
447	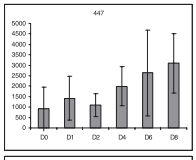	Osmotin-like protein	0.016	Disease/defense
452	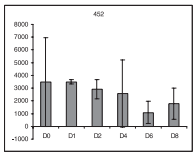	Proteinase inhibitor – Merops family I03.002	0.040	Disease/defense
453	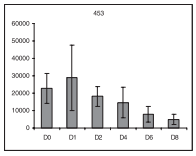	Proteinase inhibitor II - Merops family I20.001	0.017	Disease/defense
455	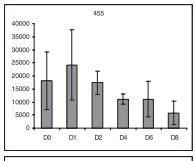	Proteinase inhibitor II – Merops family I20.001	0.041	Disease/defense
456	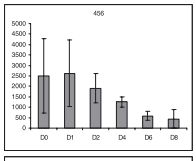	Proteinase inhibitor II – Merops family I20.002	0.019	Disease/defense
459	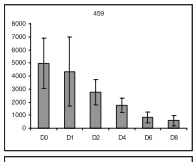	Proteinase inhibitor II – Merops family I20.001	0.001	Disease/defense
462	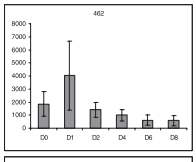	Proteinase inhibitor II precursor – Merops family I20.001	0.012	Disease/defense
464	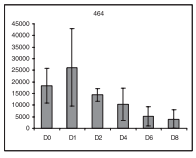	Proteinase inhibitor II precursor – Merops family I20.001	0.008	Disease/defense

Table 1. Continued

Spot number	Variation of normalised volume (affected by s.d.)	Protein identification	*p*-Value	Functional category
611	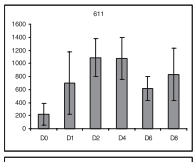	Ankyrin-repeat protein	0.000	Signal transduction
733	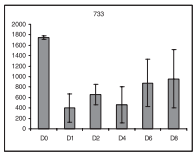	Proteinase inhibitor – Merops family I03.002	0.017	Disease/defense
762	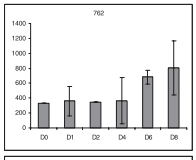	Metacaspase 1	0.000	Disease/defense
769	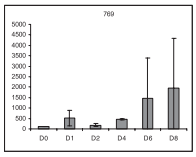	DS2 protein	0.000	Disease/defense
780	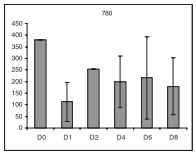	Peroxidase 1	0.026	Disease/defense
797	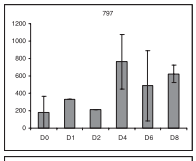	Plasma membrane polypeptide	0.005	Cell structure
810	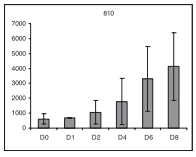	Proteinase inhibitor homologue – Merops family I03.017Patatin Protein destination and storage	0.004	Disease/defense
826	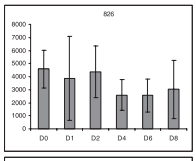	Proteinase inhibitor II – Merops family I20.001	0.026	Disease/defense
865	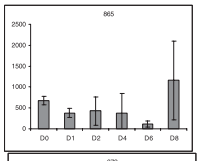	Actin	0.003	Cell structure
872	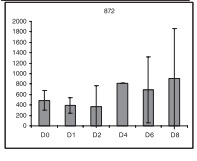	Aspartic proteinase 2	0.005	Disease/defense

Table 1. Continued

Spot number	Variation of normalised volume (affected by s.d.)	Protein identification	*p*-Value	Functional category
875	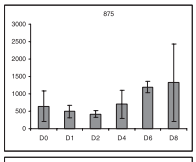	Annexin p34	0.008	Disease/defense
905	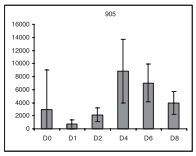	Patatin	0.031	Protein destination and storage
964	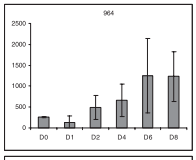	Pathogenesis-related protein STH-2	0.002	Disease/defense
969	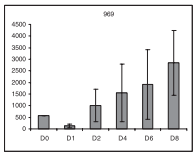	Pathogenesis-related protein STH-2	0.004	Disease/defense
1024	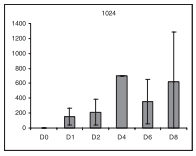	Ran protein/TC4 protein	0.031	Signal transduction
1035	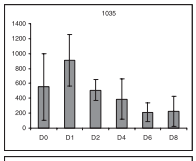	Proteinase inhibitor homologue – Merops family I03.017	0.020	Disease/defense
1067	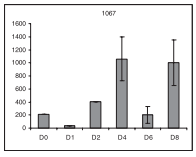	Putative mitochondrial NAD-dependent malate dehydrogenase	0.000	Energy
1076	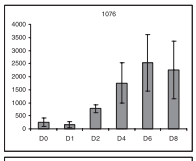	Eukaryotic initiation factor 3I1 subunit Wound-induced protein (with chitin-binding domain)	0.003	Transcription Disease/defense
1151	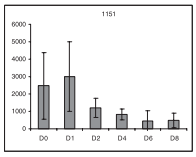	Proteinase inhibitor II – Merops family I20.001	0.026	Disease/defense
1284	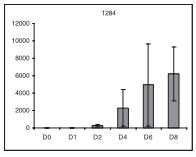	Suberisation-associated anionic peroxidase	0.005	Secondary metabolism

Table 1. Continued

Spot number	Variation of normalised volume (affected by s.d.)	Protein identification	*p*-Value	Functional category
1350	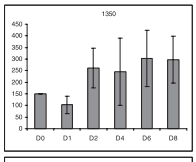	Unnamed protein product	0.007	–
1411	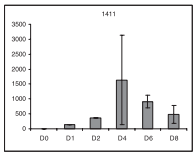	Miraculin (low homology) – Merops family I03.UNA	0.000	Disease/defense
1447	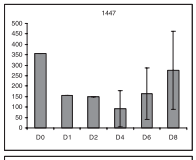	Not identified	0.011	
1450	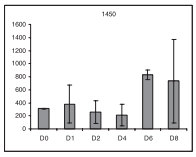	Annexin p34	0.019	Disease/defense
1458	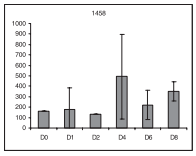	Cyprosin	0.001	Protein destination and storage
1460	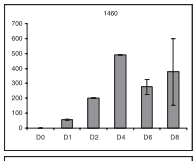	Caffeoyl-CoA 3-*O*-methyltransferase	0.000	Secondary metabolism
1462	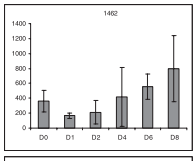	20S Proteasome alpha subunit B, putative	0.000	Protein destination and storage
1539	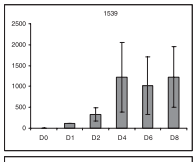	Endochitinase 1	0.004	Disease/defense
1543	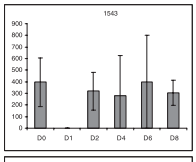	Putative transcription factor Btf3	0.040	Signal transduction
1546	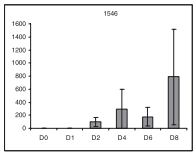	Elicitor-inducible protein EIG-J7	0.019	Disease/defense

Table 1. Continued

Spot number	Variation of normalised volume (affected by s.d.)	Protein identification	*p*-Value	Functional category
1564	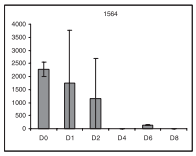	Mitochondrial malate dehydrogenase	0.001	Energy
1569	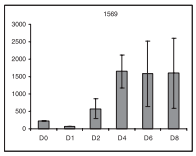	Endochitinase 2	0.001	Disease/defense
1571	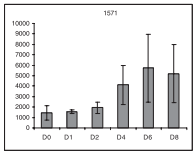	Proteinase inhibitor – Merops family I03.017	0.017	Disease/defense
1572	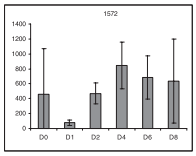	Proteinase inhibitor homologue – Merops family I03.017 Wound-induced protein (with chitin-binding domain	0.001	Disease/defense
1578	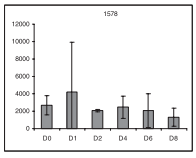	Proteinase inhibitor – Merops family I03.017	0.004	Disease/defense
		Proteinase inhibitor – Merops family I20.UPW		Protein destination and storage
1580	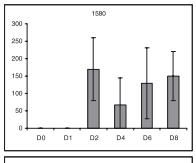	Putative ubiquitin extension protein Glutaredoxin	0.043	Disease/defense
1593	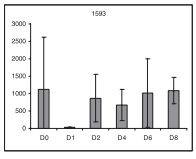	Peroxidase	0.031	Secondary metabolism
1622	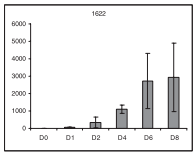	Peroxidase	0.001	Secondary metabolism
1647	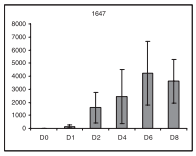	Kunitz-type protease inhibitor precursor – Merops family I20.001	0.006	Disease/defense

Table 1. Continued

Spot number	Variation of normalised volume (affected by s.d.)	Protein identification	*p*-Value	Functional category
1790	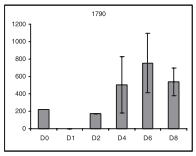	Miraculin (low homology) – Merops family I03.UNA	0.000	Disease/defense
1863	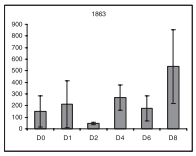	Ascorbate peroxidase	0.000	Secondary metabolism
1878	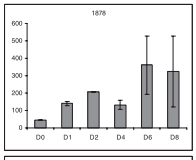	Proteinase inhibitor precursor – Merops family I03.020	0.000	Disease/defense
1929	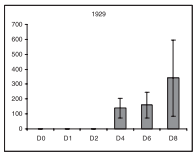	Chitinase	0.002	Disease/defense
2190	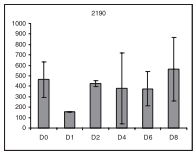	SOD [Mn], mitochondrial	0.002	Disease/defense
2275	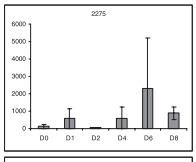	Miraculin (low homology) – Merops family I03.UNA Catalase isozyme 1-like protein	0.001	Disease/defense
2420	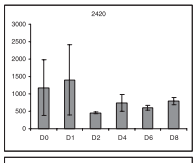	Patatin	0.001	Protein destination and storage
2458	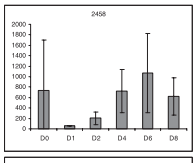	Patatin	0.004	Protein destination and storage
2464	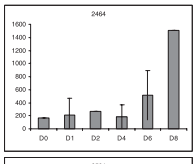	Pathogenesis-related protein 10	0.039	Disease/defense
2501	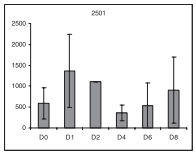	Chitin-binding lectin 1 (*not securely identified*)	0.006	Disease/defense

Table 1. Continued

Spot number	Variation of normalised volume (affected by s.d.)	Protein identification	*p*-Value	Functional category
2506	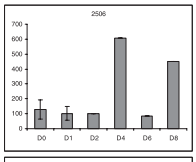	Chitin-binding lectin 1 (*not securely identified*)	0.023	Disease/defense
2510	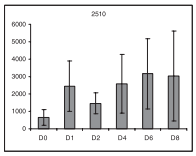	Formate dehydrogenase, mitochondrial	0.050	Energy
2511	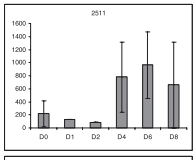	Peroxidase	0.024	Secondary metabolism
2543	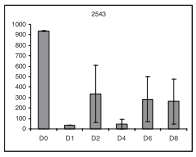	Endochitinase 1	0.003	Disease/defense
2545	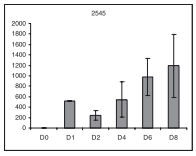	Proteinase inhibitor – Merops family I03.002	0.000	Disease/defense
2580	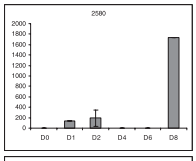	34 kDa Outer mitochondrial membrane protein porin-like protein	0.008	Disease/defense
3716	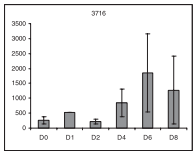	Proteinase inhibitor – Merops family I03.002	0.009	Disease/defense

3.5 Proteins from the native periderm

For identification of polypeptides from the native periderm only spots present in at least four replicates (peels from four distinct tubers) were considered and excised for MS identification (91 spots analysed and about 90% identified). The results are presented in Table 2 and Table S2 (Supporting Information material with additional information).

The major proteins that were identified can be grouped in the similar Bevan *et al.* [28] functional categories referred for the slices. Some differences between proteins identified in the slices and in the native periderm are however apparent. For instance, it seems that there is still a higher preponderance of disease/defence proteins in the periderm than in the slices, and in what concerns the protease inhibitors, the periderm has, like the slices, the Merops families I03 and I20, but members of the I13 and I25 families were additionally detected.

4 Discussion

Slicing triggers in the potato storage tissue a marked increase in respiration [18, 30] and a dedifferentiation

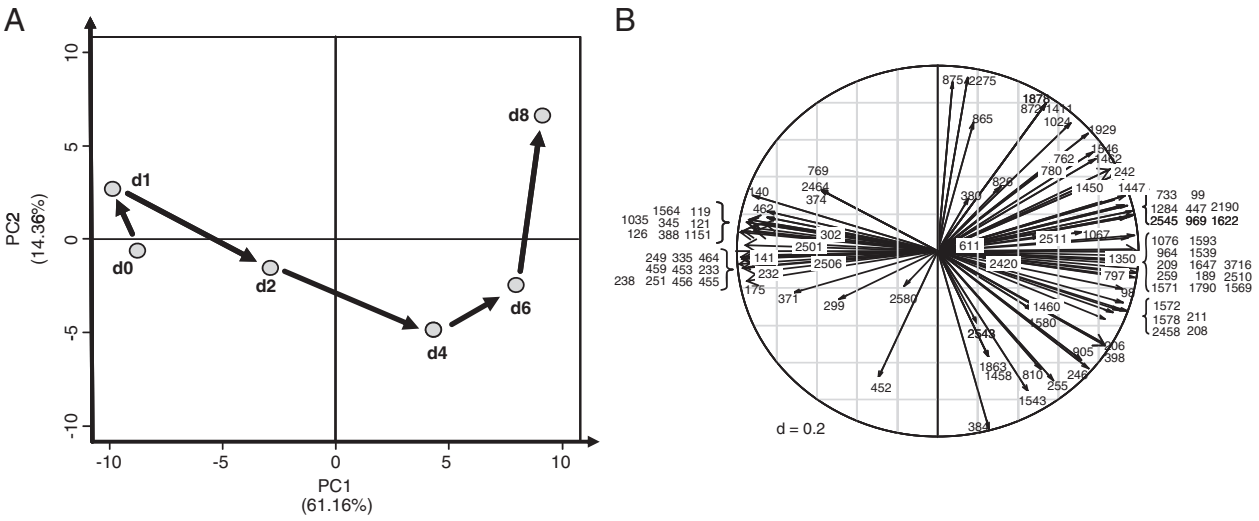

Figure 4. PCA of differentially expressed wound-induced proteins (p-value < 0.05) from potato tuber slices for sampling dates D0, D1, D2, D4, D6 and D8; (A) main plane (PC1–PC2) showing the position of the mean value resulting from analysis of the five replicate gels of each sampling date; (B) correlation circle showing the position of proteins on the PC1–PC2 plane (see spot numbering in Table 1).

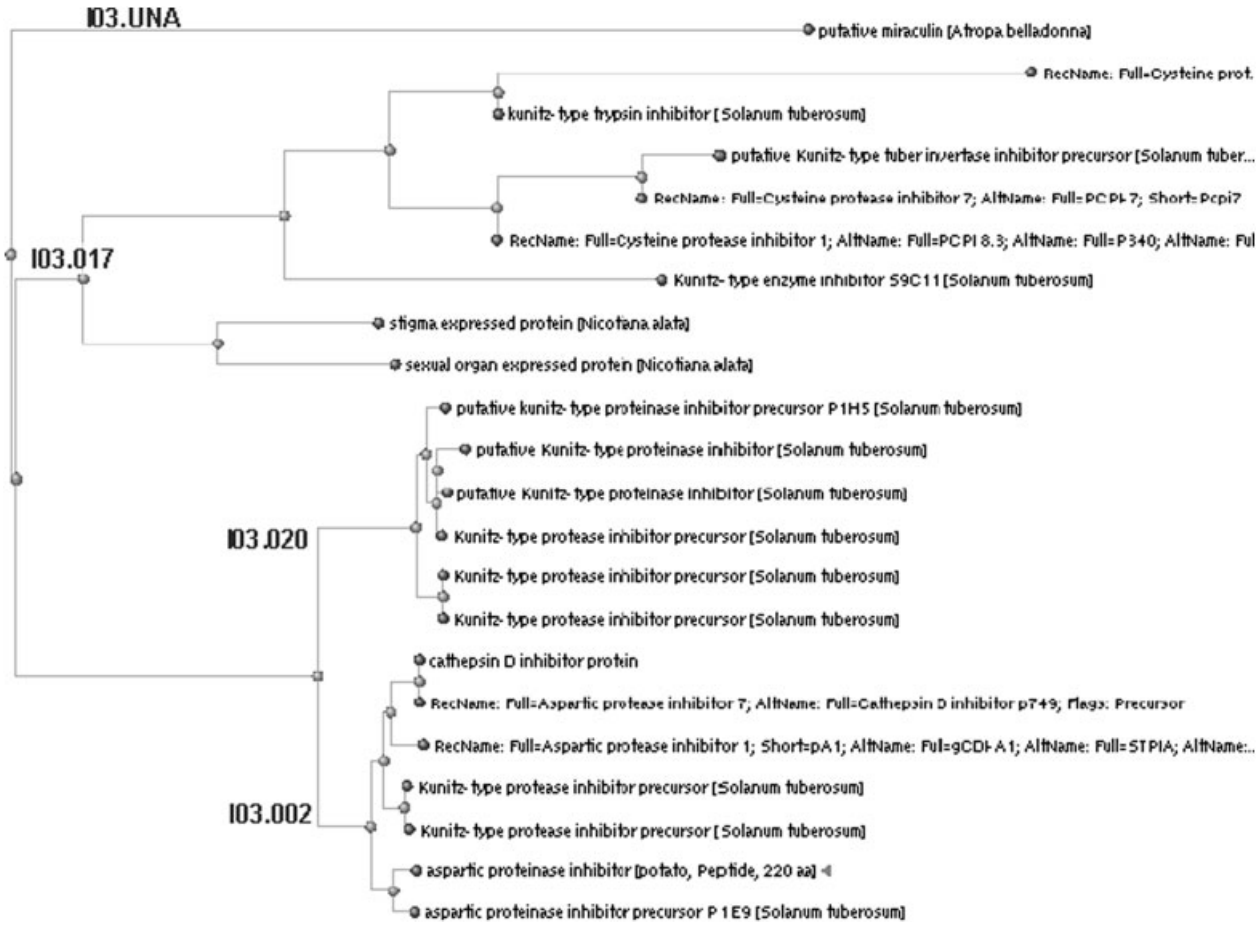

Figure 5. Distance tree (rectangle representation) for the protease inhibitors of the Merops family I03 detected in the potato slices, produced using BLAST pair-wise alignments. The Merops classification is indicated.

Table 2. Proteins from potato peels identified by MS and previously separated by 2-DE

Spot number	Protein identification	Functional category
4	Tobacco calretulin	Stress response
	26S proteasome regulatory subunit S5A	Protein destination and storage
6	Suberisation-associated anionic peroxidase 2 precursor (TMP2)	Secondary metabolism
20	Nascent polypeptide-associated complex subunit alpha-like protein 3	Intracellular traffic
33	Not identified	
40	Kunitz proteinase inhibitor homologue (sexual organ expressed protein) – Merops family I03.017	Disease/defense
	Calmodulin-5/6/7/8	Signal transduction
45	Not identified	
46	Calreticulin precursor	Protein destination and storage
47	Abscisic stress ripening protein	Transcription
48	Abscisic stress ripening protein	Transcription
70	Patatin	Protein destination and storage
72	Patatin precursor	Protein destination and storage
96	Patatin precursor	Protein destination and storage
98	Patatin precursor	Protein destination and storage
113a	Drought-induced protein sdi-6	Unclear classification
	Patatin precursor	Protein destination and storage
113b	No significant homologue found	–
114	Kunitz-type enzyme inhibitor S9C11 – Merops family I03.017	Disease/defense
115	Kunitz-type enzyme inhibitor S9C11 – Merops family I03.017	Disease/defense
116	Cysteine protease inhibitor – Merops family I03.017	Disease/defense
117	Cysteine protease inhibitor – Merops family I03.017	Disease/defense
128	Miraculin (low homology) – Merops family I03.UNA	Disease/defense
129	Miraculin (low homology) – Merops family I03.UNA	Disease/defense
	Chloroplast processing enzyme	Protein destination and storage
130	Miraculin (low homology) – Merops family I03.UNA	Disease/defense
131	Kunitz-type proteinase inhibitor – Merops family I03.020	Disease/defense
147	Proteinase inhibitor – Merops family I13.UPW	Disease/defense
148	Proteinase inhibitor – Merops family I20.UPW	Disease/defense
171	Patatin precursor	Protein destination and storage
173	Patatin precursor	Protein destination and storage
174	Patatin precursor	Protein destination and storage
175	Peroxidase 1	Secondary metabolism
177	Patatin precursor	Protein destination and storage
203	Pathogenesis-related protein 10	Disease/defense
204	Miraculin (low homology) – Merops family I03.UNA	Disease/defense
205	Pathogenesis-related protein 10	Disease/defense
	Chloroplast small heat shock protein class I	Disease/defense
206	Pathogenesis-related protein 10	Disease/defense
221	Kunitz-type enzyme inhibitor S9C11 – Merops family I03.017	Disease/defense
228	Enolase	Energy
273	Proteinase inhibitor – Merops family I03.030	Disease/defense
274	Kunitz-type protease inhibitor precursor – Merops family I03.020	Disease/defense
275	Pathogenesis-related protein 10	Disease/defense
276	Putative miraculin – Merops family I03.UNA	Disease/defense
293	Catalase	Secondary metabolism

Table 2. Continued

Spot number	Protein identification	Functional category
294	Propolyphenol oxidase	Secondary metabolism
	Catalase	Secondary metabolism
312	Formate dehydrogenase	Energy
313	Endochitinase 2 precursor	Disease/defense
314	Not identified	
331	Kunitz proteinase inhibitor homologue (sexual organ expressed protein) – Merops family I03.017	Disease/defense
332	Kunitz proteinase inhibitor homologue (sexual organ expressed protein) – Merops family I03.017	Disease/defense
358	Cold inducible; similar to other osmotic stress-induced gene products including: tomato abscisic st	Disease/defense
368	Not identified	
385	Peroxidase	Secondary metabolism
386	Peroxidase	Secondary metabolism
387	Putative mitochondrial NAD-dependent malate dehydrogenase	Energy
388	Fructose-1,6-bisphosphate aldolase	Metabolism
389	Peroxidase	Secondary metabolism
407	Osmotin-like protein	Disease/defense
408	Miraculin (low homology) – Merops family I03.UNA	Disease/defense
409	Kunitz proteinase inhibitor homologue (sexual organ expressed protein) – Merops family I03.017	Unclear classification
410	Proteasome subunit alpha type-7	Protein destination and storage
419	Putative pathogen-induced protein	Disease/defense
420	Pathogenesis-related protein	Disease/defense
421	Aspartic protease inhibitor precursor	Disease/defense
436	Cold inducible; similar to other osmotic stress-induced gene products including: tomato abscisic st	Disease/defense
448	Peroxidase	Secondary metabolism
449	Propolyphenol oxidase	Secondary metabolism
452	Peroxidase	Secondary metabolism
471	Endochitinase 4 precursor	Disease/defense
472	Peroxidase	Secondary metabolism
473	Peroxidase	Secondary metabolism
474	Peroxidase precursor	Secondary metabolism
	Glyceraldehyde 3-phosphate dehydrogenase	Energy
475	Peroxidase	Secondary metabolism
476	Glucan endo-1,3-beta-glucosidase	Metabolism
477	Peroxidase	Secondary metabolism
481	Porin	Transporters
	1,3-Beta-glucan glucanohydrolase	Metabolism
516	Cysteine protease inhibitor precursor – Merops family I03.017	Disease/defense
517	Aspartic proteinase inhibitor precursor – Merops family I03.002	Disease/defense
518	Kunitz-type protease inhibitor precursor – Merops family I03.020	Disease/defense
539	Kunitz-type trypsin inhibitor – Merops family I03.017	Disease/defense
557	Peroxidase	Secondary metabolism
558	Putative peroxidase	Secondary metabolism
559	Polygalacturonase inhibitor protein	Disease/defense
561	Peroxidase precursor	Secondary metabolism
581	Peroxidase	Secondary metabolism
	Glucan endo-1,3-beta-glucosidase	Metabolism
582	Peroxidase	Secondary metabolism
583	Endochitinase 1 precursor	Disease/defense
585	Acid phosphatase	Metabolism
596	Putative Kunitz-type tuber invertase inhibitor precursor – Merops family I03.017	Disease/defense
597	Cysteine protease inhibitor – Merops family I03.002	Disease/defense
598	Psmotin-like protein OSML81 precursor	Disease/defense
616	Cyclophilin	Signal transduction
	Aspartic protease inhibitor – Merops family I03.002	Disease/defense

Table 2. Continued

Spot number	Protein identification	Functional category
617	Pathogenesis-related protein PR-1 precursor	Disease/defense
627	Kunitz proteinase inhibitor homologue (stigma expressed protein) – Merops family I03.017	Disease/defense
630	Cystatin	Disease/defense
	Putative non-specific lipid transfer protein	Disease/defense
	Probable protease inhibitor P322 precursor	Disease/defense
631	Probable protease inhibitor P322 precursor	Disease/defense
681	Plant basic secretory protein	Disease/defense

process [18, 31] with formation of a wound-periderm [5], which involves the activation of many genes. In general terms we can consider that the alterations in the slices proteins that we are here reporting are related to those profound changes in metabolism that are triggered by excision. The PCA representation clearly shows a progression of interrelated events defining two major groups of the sampling dates (D0, D1, D2 and D4, D6, D8), which suggests a sequence of metabolic process occurring with time. Interestingly, by applying a PCA to non-polar metabolite profiles of potato slices, Yang and Bernards [32] also observed a progression of changes with time that defined three main clusters (D0–D2, D3–D4 and D5–D7).

The storage proteins of the potato tuber should have a marked contribution to the wound induced events. Patatins and protease inhibitors form the bulk of the tuber protein and are mostly considered to be storage proteins [33]. The high MW forms of patatins we detect at D0–D1 (steadily decreasing to D8) and the lower MW forms of D4–D6 have similar sequences, which suggests that these last ones are mainly degradation products of the tuber patatins. About their role in the cell, patatins are mainly localised in the vacuoles, where they are inactive, but cytosolic forms with lipid acyl-hydrolase activity were detected [34] and there are indications they have other enzymatic activities and participate in resistance reactions induced by pathogen attack [35].

Regarding the protease inhibitors, they also form a numerous group of proteins in the slices. The fact that the different classes detected have distinct expression patterns along the sampling dates suggests that they may have complex and marked roles during the wound-healing process. Their participation in defence and in the regulation of proteolysis associated with development could be proposed. Induction in response to wounding was referred [36, 37], as well as involvement in several developmental processes, such as programmed cell death [38]. A complexity of functions for the inhibitors in the wound-healing process is further stressed by the presence in the native periderm of two families (I13 and I25) that we did not detect in the slices. These two families of inhibitors have been considered to be important in pathogen defence [39].

Of the several responses activated by wounding, suberisation is certainly of great significance since suberin deposition in the cell wall acts as a physical barrier against water movement and pathogen attack [1, 3]. At D4 the polyaliphatic domain of the suberin layer was already evident, which agrees with the Lulai and Corsini [40] report that the tubers acquired total resistance to fungal infection from the 5th to the 7th day after wounding, when complete deposition of the suberin aliphatic domain on the 1st cell's layer was reached. Some of the proteins expressed in the D6–D8 slices are similar to proteins detected in the native periderm (including a suberisation-associated anionic peroxidase), which suggests that the slice metabolism in the later stages tends to acquire similarities to that of the native periderm. However, the gel patterns of the two tissues still differed and it is possible that a higher similarity could be reached at a later stage. In fact, Stark *et al.* [5] stated that periderm formation in the potato slices is an extended process that continues for at least 14 days, with the deposition of aliphatic long-chain species dominating from the 7th day onwards. Nevertheless, it is interesting to find that both histological observations and immunolabelling analyses indicate that there are differences in the cell walls of wound *versus* native periderm [3].

ROS that are known to be produced in association with stress (oxidative burst) play a central role in wound response [41], and at least four successive peaks of oxidative burst were observed in association with potato wounding [42]. ROS have a dual nature, being cytotoxic exacerbate damage but, at the same time, have a key role in regulation of defence mechanisms [41] by activating genes, for instance of the phenylpropanoid pathway [43], and by participating in pathogen response [10]. Plants have very efficient antioxidant defence systems either enzymatic or non-enzymatic, which allow scavenging of ROS and protection of cells against oxidative damage [44].

GST is an important protein in cell protection against ROS, being responsible for the complexation of GSH to a variety of compounds later subjected to cellular detoxification. The identification of GST forms, one with a maximum of expression during D4–D8, suggests a very important role for GST throughout the slice wound-healing process. The presence of superoxide dismutase (SOD), glutaredoxin and

catalases is also significant when considering protection from ROS.

The activation of inducible defence mechanisms that result in the production of a diversity of antimicrobial compounds, such as phenols [45] and peptides (*e.g.* PR and PR-like proteins) [6], is also of crucial importance during the wound-healing process. Several proteins belonging to some of the 19 groups of PR families [6], were also detected: beta-1,3-glucanase (PR-2); chitinases (PR-3); osmotins (PR-5); protease inhibitors (PR-6); plant peroxidases (PR-9); PR-10 proteins. This observation indicates that PR proteins are greatly implicated in the metabolic changes that occur upon slicing. It is known that they are strongly induced by wounding or infection (fungal, bacterial or viral) and that they contribute to plant defence [46] but, in addition, participate in many physiological and developmental processes, including embryogenesis and abscission [6]. The fact that these proteins are well represented during D4–D8 indicates a role in the later stages of wound-healing, such as protection and cell-wall reconstruction (see Lulai [3]). Noticeably, many disease/defence proteins were also detected in the native periderm, in agreement with a previous report [16], stressing the protective function of that structure.

Secondary metabolites also play a crucial role in many plant processes and their synthesis should be intensified during the healing reconstruction in the slices. Important compounds such as, lignin, suberin, wall-bound phenolics and flavonoids derive their building units from the phenylpropanoid pathway and are important in defence and tissue reconstruction [47, 48]. The identification of caffeoyl-CoA methyltransferase and several peroxidases is of relevance. The peroxidases detected during D4–D8 could, in addition to a defence role, participate in the crosslinking of the hydroxycinamic alcohols that constitute lignin and the polyphenolic domain of suberin [49, 50]. The detection of a suberisation-associated anionic peroxidase, also present in the native periderm, supports the observation of cell-wall strengthening during the wound-healing process.

Additional information on the succession of events leading to slice healing is given by the identification of proteins participating in other important metabolic processes, such as carbohydrate metabolism, transport, transcription, signal transduction and cell structure. For instance, the identification of metacaspase, proteosoma sub-units and polyubiquitin reinforces the importance of proteolysis in these processes, also indicated by the presence of the protease inhibitors. Furthermore, identification of actin and annexin is indicative of profound alterations in cellular metabolism, with emphasis on cell structure reorganisation, since annexin is known to participate in Ca^{2+}-dependent intracellular signaling, Golgi-mediated polysaccharide segregation and in the interaction with several cellular compounds involved in cell organisation [51, 52].

In conclusion, we present proteomic evidence for the wound-healing mechanisms of potato tissue and highlight the succession of several interrelated phases where different classes of proteins participate. The data add information for a more comprehensive picture of these processes. The important roles for some proteins are indicated, but their precise function needs to be investigated in detail in order to recognise well the key steps of the healing mechanisms in plants. Since potato slices are a good model system to study suberin formation, this work could be useful as a starting point for a broader goal that is the study of suberin and cork formation.

The technical skills of Isabel Martins and Ana Margarida Santos in the microscopic observations of the slices are acknowledged. This work was supported by project FCT/POCTI/39011/AGR/2001. I.C. acknowledges an FCT grant (SFRH/BPD/20833/2004).

The authors have declared no conflict of interest.

5 References

[1] Kolattukudy, P. E., Biopolyester Membranes of Plants: Cutin and Suberin. *Science* 1980, *208*, 990–1000.

[2] Sabba, R. P., Lulai, E. C., Histological analysis of the maturation of native and wound periderm in potato (*Solanum tuberosum* L.) tuber. *Annals of Botany* 2002, *90*, 1–10.

[3] Lulai, E., Skin-Set, Wound Healing, and Related Defects, in: Vreugdenhil, D. (Ed.), *Potato Biology and Biotechnology: Advances and Perspectives*, Elsevier BV 2007.

[4] Fry, S., Cross-linking of matrix polymers in the growing cell walls of angiosperms. *Annu. Rev. Plant Physiol.* 1986, *37*, 165–186.

[5] Stark, R. E., Sohn, W., Pacchiano,R. A., Jr., Al-Bashir, M., Garbow, J. R., Following suberization in potato wound periderm by histochemical and solid-state 13C nuclear magnetic resonance methods. *Plant Physiol.* 1994, *104*, 527–533.

[6] van Loon, L. C., Rep, M., Pieterse, C. M. J., Significance of inducible defense-related proteins in infected plants. *Annu. Rev. Phytopathol.* 2006, *44*, 135–162.

[7] Bowles, D. J., Defense-related proteins in higher plants. *Annu. Rev. Biochem.* 1990, *59*, 873–907.

[8] Richards, H. M., The respiration of wounded plants, with woodcuts 2 and 3. *Ann. Bot.* 1896, *10*, 531–583.

[9] Rees, T. A., Beevers, H., Pentose phosphate pathway as a major component of induced respiration of carrot and potato slices. *Plant Physiol.* 1960, *35*, 839–847.

[10] Zhou, L., Thornburg, R. W., in: Reynolds, P., (Ed.), *Inducible Gene Expression in Plants*, CAB International, Wallingford, UK 1999, pp. 127–167.

[11] Gallardo, K. C. S., Vandekerckhove, J. R. T., Burstin, J., Proteomics of Medicago truncatula seed development establishes the time frame of diverse metabolic processes related to reserve accumulation. *Plant Physiol.* 2003, *133*, 664–682.

[12] Abbasi, F., Komatsu, S., A proteomic approach to analyze salt-responsive proteins in rice leaf sheath. *Proteomics* 2004, *4*, 2072–2081.

[13] Zhu, H., Bilgin, M., Snyder, M., Proteomics. *Annu. Rev. Biochem.* 2003, *72*, 783–812.

[14] Ippel, J., Pouvreau, L., Kroef, T., Gruppen, H. *et al.*, *In vivo* uniform 15N-isotope labelling of plants: using the greenhouse for structural proteomics. *Proteomics* 2003, *4*, 226–234.

[15] Satu, J., Lehesranta, S., Davies, H., Shepherd, L. *et al.*, Comparison of tuber proteomes of potato varieties, landraces, and genetically modified lines. *Plant Physiol.* 2005, *138*, 1690–1699.

[16] Barel, G., Ginzberg, I., Potato skin proteome is enriched with plant defence components. *J. Exp. Bot.* 2008, *59*, 3347–3357.

[17] Delaplace, P., Fauconnier, M. L., Sergeant, K., Dierick, J. F. *et al.*, Potato (*Solanum tuberosum* L.) tuber ageing induces changes in the proteome and antioxidants associated with the sprouting pattern. *J. Exp. Bot.* 2009, *60*, 1273–1288.

[18] Laties, G. G., Controlling influence of thickness on development and type of respiratory activity in potato slices. *Plant Physiol.* 1962, *37*, 679–690.

[19] Krishnamurthy, K. V., *Methods in Cell Wall Cytochemistry*, Humana Press, New Jersey 1999.

[20] Ramagli, L. S., in: Link, A. J. (Ed.), *Methods in Molecular Biology*, Humana Press, New Jersey 1999, pp. 95–105.

[21] Neuhoff, V., Stamm, R., Eibl, H., Clear background and highly sensitive protein staining with coomassie blue dyes in polyacrylamide gels: a systematic analysis. *Electrophoresis* 1985, *6*, 427–448.

[22] Smyth, G. K., in: Gentleman, R., Carey, V., Dudoit, S., Irizarry, R., Huber, W. (Eds.), *Bioinformatics and Computational Biology Solutions using R and Bioconductor*, Springer, New York 2005, pp. 397–420.

[23] Benjamini, Y., Hochberg, Y., Controlling the false discovery rate-a practical and powerful approach to multiple testing. *J. R. Stat. Soc. Series B* 1995 *57*, 289–300.

[24] Chessel, D., Dufour, A. B., Thioulouse, J., The ade4 package-I-One-table methods. *R news* 2004, *4*, 5–10.

[25] Bohler, S., Bagard, M., Oufir, M., Planchon, S. *et al.*, A DIGE analysis of developing poplar leaves subjected to ozone reveals major changes in carbon metabolism. *Proteomics* 2007, *7*, 1584–1599.

[26] Mackey, A., Haystead, T., Pearson, W., Getting more from less: algorithms for rapid protein identification with multiple short peptide sequences. *Mol. Cell. Proteomics* 2002, *1*, 139–147.

[27] Samyn, B., Sergeant, K., Carpentier, S., Debyser, G. *et al.*, Functional proteome analysis of the banana plant (Musa spp.) using de novo sequence analysis of derivatized peptides. *J. Proteome Res.* 2007, *6*, 70–80.

[28] Bevan, M., Bancroft, I., Bent, E., Love, K. *et al.*, Analysis of 1.9 Mb of contiguous sequence from chromosome 4 of Arabidopsis thaliana. *Nature* 1998, *391*, 485–488.

[29] Rawlings, N., Morton, F., Kok, C., Kong, J., Barrett, A., MEROPS: the peptidase database. *Nucleic Acids Res.* 2008, *36*, D320–D325.

[30] Wadso, L., Gomezb, F., Sjöholmb, I., Rocculic, P., Effect of tissue wounding on the results from calorimetric measurements of vegetable respiration. *Thermochim. Acta* 2004, *422*, 89–93.

[31] Fabbri, A. A., Fanelli, C., Reverberi, M., Ricelli, A. *et al.*, Early physiological and cytological events induced by wounding in potato tuber. *J. Exp. Bot.* 2000, *51*, 1267–1275.

[32] Yang, W., Bernards, M. A., Metabolomic Analysis of wound-induced suberization in potato (*Solanum tuberosum L.*) tubers. *Metabolomics* 2007, *3*, 147–159.

[33] Bauw, G., Nielsen, H. V., Emmersen, J., Nielsen, K. L. *et al.*, Patatins, Kunitz protease inhibitors and other major proteins in tuber of potato cv. Kuras. *FEBS J.* 2006, *273*, 3569–3584.

[34] Hirschberg, H. J. H. B., Simons, F. A. J., Dekker, N., Egmond, M. R., Cloning, expression, purification and characterization of patatin, a novel phospholipase A. *Eur. J. Biochem.* 2001, *268*, 5037–5044.

[35] Kumar, G. N. M., Houtz, R. L., Knowles, N. R., Age-induced protein modifications and increased proteolysis in potato seed-tubers. *Plant Physiol.* 1999, *119*, 89–99.

[36] Major, I. T., Constabel, C. P., Functional analysis of the Kunitz trypsin inhibitor family in poplar reveals biochemical diversity and multiplicity in defense against herbivores. *Plant Physiol.* 2008, *146*, 888–903.

[37] Gruden, K., Strukelj, B., Popovic, T., Lenarcic, B. *et al.*, The cysteine protease activity of Colorado potato beetle (*Leptinotarsa decemlineata* Say) guts, which is insensitive to potato protease inhibitors, is inhibited by thyroglobulin type-1 domain inhibitors. *Insect Biochem. Mol. Biol.* 1998, *28*, 549–560.

[38] Solomon, M., Belenghi, B., Delledone, M., Meachem, E., Levine, A., The involvement of cysteine proteases inhibitor genes in the regulation of programmed cell death in plants. *Plant Cell* 1999, *11*, 431–443.

[39] Habib, H., Fazili, K. M., Plant protease inhibitors: a defense strategy in plants. *Biotechnol. Mol. Biol. Rev.* 2007, *2*, 68–85.

[40] Lulai, E. C., Corsini, D. L., Differential deposition of suberin phenolic and aliphatic domains and their roles in resistance to infection during potato tuber *(Solanum tuberosum L.)* wound-healing. *Physiol. Mol. Plant Pathol.* 1998, *53*, 209–222.

[41] Foyer, C., Noctor, G., Oxidant and antioxidant signalling in plants: a re-evaluation of the concept of oxidative stress in a physiological context. *Plant Cell Environ.* 2005, *28*, 1056–1071.

[42] Razem, F., Bernards, M., Reactive oxygen species production in association with suberization: evidence for an NADPH-dependent oxidase. *J. Exp. Bot.* 2003, *54*, 935–941.

[43] Saltveit, M. E., Choi, Y. J., Tomas-Barberan, F. A., Involvement of components of the phospholipid-signaling pathway in wound-induced phenylpropanoid metabolism in lettuce (*Lactuca sativa*) leaf tissue. *Physiol. Plantarum* 2005, *125*, 345–355.

[44] Vranová, E., Inzé, D. F. V. B., Signal transduction during oxidative stress. *J. Exp. Bot.* 2002, *53*, 1227–1236.

[45] Bowles, D., Signal transduction in the wound response of tomato plants. *Phil. Trans. Roy. Soc. Lond. B Biol. Sci.* 1998, *353*, 1495–1510.

[46] Van Loon, L. C., Van Strien, E. A., The families of pathogenesis-related proteins, their activities, and comparative analysis of PR-1 type proteins. *Physiol. Mol. Plant Pathol.* 1999, *55*, 85–97.

[47] Hayashi, M., Takahashi, H., Tamura, K., Huang, J. *et al.*, Enhanced dihydroflavonol-4-reductase activity and NAD homeostasis leading to cell death tolerance in transgenic rice. *Proc. Natl. Acad. Sci. USA* 2005, *102*, 7020–7025.

[48] Xie, D.-Y., Jackson, L. A., Cooper, J. D., Ferreira, D., Paiva, N. L., Molecular and biochemical analysis of two cDNA clones encoding dihydroflavonol-4-reductase from Medicago truncatula. *Plant Physiol.* 2004, *134*, 979–994.

[49] Bernards, M. A., Demystifying suberin. *Can. J. Bot.* 2002, *80*, 227–240.

[50] Lewis, N. G., Yamamoto, E., Lignin: occurrence, biogenesis and biodegradation. *Annu. Rev. Plant Physiol. Plant Mol. Biol.* 1990, *41*, 455–496.

[51] Delmer, D. P., Potikha, T. S., Structures and functions of annexins in plants. *Cell. Mol. Life Sci.* 1997, *53*, 546–553.

[52] Hofmann, A., Annexin in the plant kingdom: perspectives and potentials. *Annexins* 2004, *1*, 51–61.

